IEEE Access
Multidisciplinary | Rapid Review | Open Access Journal

Received February 18, 2022, accepted March 12, 2022, date of publication March 16, 2022, date of current version March 24, 2022.

Digital Object Identifier 10.1109/ACCESS.2022.3159791

A Dual Slant-Polarized Cylindrical Array of Tightly Coupled Dipole Antennas

XIANYANG LV[1,2], YONGWEI ZHANG[1], (Member, IEEE), QUAN SHI[1], MURAT TEMIZ[3], (Member, IEEE), AND AHMED EL-MAKADEMA[4]

[1]School of Transportation, Nantong University, Nantong, Jiangsu 226019, China
[2]School of Information Science and Technology, Nantong University, Nantong, Jiangsu 226019, China
[3]Department of Electronic and Electrical Engineering, University College London, London WC1E 7JE, U.K.
[4]Department of Electrical and Electronic Engineering, The University of Manchester, Manchester M13 9PL, U.K.

Corresponding author: Yongwei Zhang (david.y.zhang@ntu.edu.cn)

This work was supported in part by the National Natural Science Foundation of China under Grant 62174091, in part by the Postgraduate Research and Practice Innovation Program of Jiangsu Province under Grant KYCX20-2792, and in part by the Postdoctoral International Exchange Program YJ20210098.

ABSTRACT This study proposes a design of a low-profile ultra wide-band cylindrical antenna array with plus/minus 45-degree dual polarization. The proposed compact cylindrical antenna array produces an omnidirectional radiation pattern in the azimuth plane to cover all directions. It consists of 20 × 4 dual-polarized elements within a diameter of 131 mm and a height of 116 mm. The array elements are tightly coupled slant-polarized wideband dipole antennas, and hence, rotational symmetry of radiation patterns in the horizontal plane is achieved for the two orthogonal polarizations. Furthermore, a metasurface structure has been designed and placed over the interconnected array elements to achieve ultrawideband capabilities. The proposed array provides less than −10 dB reflection coefficient over a frequency band between 1.7 GHz and 5.9 GHz. The cross-polarization discrimination (XPD) is 15 dB at boresight in the azimuth plane. The electromagnetic characteristics of the cylindrical array and its corresponding planar array before bending have been evaluated and compared via simulations, and verified by measurements. The compact size, lightweight, and printable design of the proposed antenna array enable low-cost manufacturing and ease of installation. The proposed array design overcomes many challenges encountered in wide-band MIMO systems by covering the entire sub-6 GHz band while providing wide 360-degree coverage in the azimuth plane, hence, supporting multibeam applications.

INDEX TERMS Cylindrical arrays, frequency selective surfaces, phased arrays, planar arrays, ultrawideband antennas.

I. INTRODUCTION

Beamforming are becoming increasingly important in the fields of communication, sensing, and imaging. In addition, low-profile, broad bandwidth, polarization diversity and wide coverage are also important to maximize performance [1]–[4]. Conformal antenna arrays can meet these requirements in addition to allowing easy integration on a curved surface [5], [6]. Cylindrical array is one of such examples that can provide an omnidirectional coverage in the azimuth while achieving high directivity in the elevation plane. The radiation pattern of the cylindrical array can be further manipulated by splitting the entire antenna array surface into sectors for multi-beams, using flexible feeding networks and fitting onto a predefined shape [7].

Polarization diversity is one of the key aspects to boost the system performance by providing a diversity between the polarizations [8]. Unlike planar antenna arrays, where the surface of the radiators spread uniformly in every direction, the surface curvature for the elements in the cylindrical array varies with direction. For example, sharp bending in the horizontal plane while no bending in the vertical plane. This leads to nonidentical radiation patterns for dual polarized elements if they are orthogonally polarized in the horizontal and vertical planes. Dual polarization based on ±45° over the cylindrical surface can solve this problem by

The associate editor coordinating the review of this manuscript and approving it for publication was Mohammed Bait-Suwailam.

This work is licensed under a Creative Commons Attribution 4.0 License. For more information, see https://creativecommons.org/licenses/by/4.0/

providing uniform patterns in both planes since the two ±45° polarizations are altered in the same way by the curvature. The identical polarized patterns in horizontal and vertical planes of the ±45° polarized antenna ensure low coupling and thus low correlation in the horizontal plane. Hence, its polarization diversity is more competitive compared to antennas of vertical or horizontal polarization in typical urban-suburban radio environments [9].

Tightly coupled dipole antenna (TCDA) has been widely considered as an approximation implementation of the current sheet model [10]–[12]. It is a low-profile, light-weight, planar design with wideband capability. However, the total thickness of the array is limited by the distance from the ground plane. The minimum thickness for TCDA is reported as slightly shorter than a half wavelength of the highest operational frequency. This is based on the initial concept presented by Munk [13]. A capacitive coupling is introduced between the elements to counter the inductive effect of the ground plane at lower frequencies. A crossed ring structure in conjunction with a metamaterial layer is later found to achieve a broader bandwidth, while maintaining the low-profile structure [14], [15].

The introduction of tip-end capacitance in the dipole array increases the bandwidth by a certain degree, but not sufficiently wide enough, especially when the array is scanned to wide angles from boresight. The conventional solution to this problem is to use wide-angle impedance matching (WAIM) structures made up of a stack of dielectric layers [16]. However, this method potentially introduces an extra loss into the system and it is not cost-effective. Much greater flexibility may be achieved by employing anisotropic slabs with controllable spatial dispersivity. Artificially structured materials (such as metamaterials or metasurfaces) make this approach feasible by allowing the simultaneous control of dielectric and magnetic properties in different directions [17]. A metamaterial layer formed by array of conductive disks was used in this study to ensure that the array can operate over the entire 5G sub-6 GHz band for mobile communication.

Polarization purity of the TCDA or the interconnected cross ring antenna is satisfactory as this structure is essentially originated from a dipole structure. In a planar array structure, this feature is preserved and the radiations patterns of both polarizations are identical for orthogonally polarized two elements. In a cylindrical array configuration, the dual polarized elements are bent differently if they are polarized in the horizontal or vertical planes. Hence the radiation patterns of two polarizations vary significantly in azimuth plane, leading to an asymmetry between the two polarizations. However, in the case of employing ±45° polarized elements, the radiation patterns of both polarizations are identical even after the array plane becomes deformed on a cylindrical surface. As a result, this study adopted ±45° dual polarized elements to establish the array and provide uniform azimuth coverage for the two orthogonal polarizations.

Dual polarization of ±45° is also expected to combat multipath and other scattering propagation effects present in modern mobile communication systems, by offering symmetrical propagation characteristics [18]. Cross-polarization discrimination (XPD) is widely used to evaluate the polarization performance. As a rule of thumb, the desired XPD is at least 20 dB at boresight and 10 dB in the range of main beams. However, this requirement becomes increasingly more stringent as more ports are introduced in antenna arrays. As indicated in [19], there are not sufficient studies on ±45° polarized antennas, and parasitic elements have been placed around the dual polarized element to enhance the XPD performance. Studies on slant polarized arrays on a curved surface were even less covered. For an antenna array of dual polarization, it is equally important to achieve symmetrical radiation patterns for dual polarization while maintaining a reasonable XPD performance across the main lobe in azimuth plane.

An omnidirectional radiation pattern is required to cover the entire surrounding of the antenna array for wireless communication networks. The cylindrical array structure produces this omnidirectional coverage in the azimuth plane while each antenna pair provides uniform dual polarization of ±45°, i.e., slant polarization, with a reasonable XPD. There are very few publications about slanted omnidirectional antennas of ultrawide bandwidth. In [20], a ±45° polarized omnidirectional antenna operational between 1.9 GHz and 2.2 GHz is introduced, with the XPD at 15 dB. A method to enhance cross polarization performance of a ±45° slant-polarized antenna is reported in [19] where XPD is more than 20 dB at boresight and 10 dB within ±45° off the boresight direction.

Massive multiple-input-multiple-output (MIMO) is one of the key technologies to achieve huge data rates in 5G and beyond communication networks since it exploits spatial diversity to communicate with multiple users within the same time-frequency resources [21], [22]. However, the antenna array design and its features have an impact on the channel correlation among users, and hence, effecting the capacity of massive MIMO communication channels [23]. These design features include radiation pattern, mutual coupling, array gain, bandwidth and total efficiency, that are highly critical to the overall performance of massive MIMO communication systems. The proposed antenna array is a potential solution for wideband massive MIMO base stations as it provides a nearly ommnidirectional radiation pattern and a dual polarization with a satisfactory discrimination between the two polarizations, resulting in a low channel correlation between them. Moreover, it is shown that cylindrical arrays perform satisfactorily in massive MIMO base stations while occupying a relatively smaller space [24].

In this paper, the properties of the cylindrical array formed by tightly coupled dipole antennas of slanted ±45° polarization were investigated. The cylindrical antenna array curvature was transformed from a slanted square grid based

planar array. The planar array antenna was manufactured first and rolled into a cylindrical shape by connecting the two ends, filled up with expandable polyethylene foam between the center ground plane tube and the curved surface of the antenna array. Both the cylindrical array antenna and its corresponding planar array antenna have the same ±45° polarization and consist of the same number of antenna elements.

To access the array elements for measurement and characterization, a bended coplanar waveguide (CPW) design has been used for feeding. The CPW strip was made flexible by using thin microwave substrate. The TCDAs have been fed with a single-ended feed structure [25], [26] or through a balanced feedline [27], [28]. Folded or perforated Marchand balun have been recently used to feed the TCDAs in [29], [30]. These designs add a complex structure between array surface and ground plane, hence, require complicated fabrication process. The CPW feeding method was adopted for its relative simplicity. In order to avoid crossover of the two feed lines for dual polarization at the array surface, the elements for ±45° polarization were designed in offset position vertically, and manufactured on the opposite side of the same board.

The rest of the article is organized as follows. In Section II, the full cylindrical array model was established, analyzed and compared with its correspondent planar array, experimental verification is presented in Section III, discussion is in Section IV, and Section V draws the conclusion.

II. CYLINDRICAL ARRAY DESIGN

The overall structure and fundamental layers of the proposed cylindrical array are depicted in Fig. 1. This cylindrical array design is achieved by wrapping up a planar array around a cylinder. The planar array and the associated unit cell model is illustrated in Fig. 2, which consists of three conductive layers. The active antenna layer is composed of dual polarized antenna elements in the middle, which is backed up by a ground plane within a proper distance, and a metasurface layer is placed over the active antenna layer. The substrate for the metasurface is ultrathin polyimide (PI) film with a thickness of 25 μm and the substrate for the antenna elements is a thin Polytetrafluoroethylene (PTFE) board with a thickness of 0.254 mm. The elements polarized in +45° are placed on one (top) side of the board and the elements of −45° polarization are placed on the opposite side (bottom) of the same substrate. The polarization directions are orthogonal to each other. The unit cell of the dual polarized elements in the array is illustrated in Fig. 2(b). The basic building block of the array can be considered as dual polarized wideband dipoles (crossed disks) with an enhanced coupling between them and a metasurface layer is formed by conductive disks following the same pattern as the elements in the array. For the planar array operating between 1.7 and 5.9 GHz, the optimal element spacing is 26 mm ($L + F = 26$ mm), the distance between the array surface and the ground plane is 16 mm, and the separation between the planar array and the metasurface

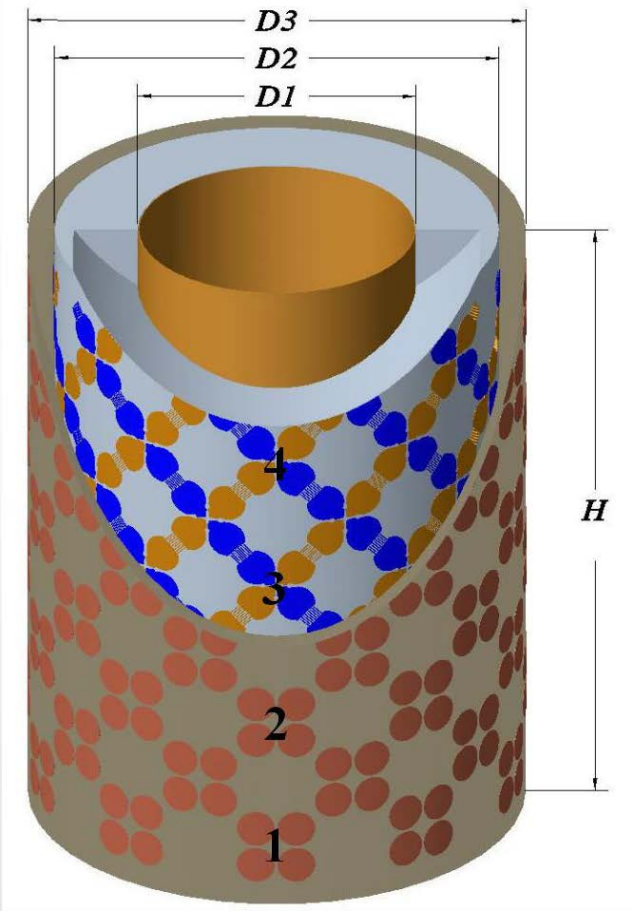

FIGURE 1. The proposed ±45° dual polarized cylindrical antenna array, consisting of 20 columns and 80 elements in each polarization, the elements "1," "2," "3," and "4" form one of the 20 columns.

is 7 mm. The optimum capacitance of the capacitor between two adjacent elements in the proposed array design is 0.34 pF. The parameters for the unit cell design and the physical dimension of the cylindrical array with the target frequency band between 1.7 and 5.9 GHz are given in Table 1 and Table 2.

A. INPUT IMPEDANCE ANALYSIS

For an infinite current sheet in free space with infinitesimal "unit cell" radiators, infinite operational bandwidth and frequency-independent behaviour were demonstrated [31], where the scanning radiation impedance within the whole visible space ($u^2 + v^2 \leq 1$) is given by

$$Z_{X(Y)}(u, v) = \eta_0(1 - t^2)/w, \tag{1}$$

where t stands for the x- and y-polarized currents in $(u, v, w) = \sin\theta\cos\phi, \sin\theta\sin\phi, \cos\theta$ domain, η_0 is the wave impedance in free space. No reactance component exists in (1). Hence, this expresses infinite bandwidth in theory. In conformal arrays, a practical backing plane is necessary. However, placing an electric conductor next to the current sheet limits its bandwidth. In fact, a conductor

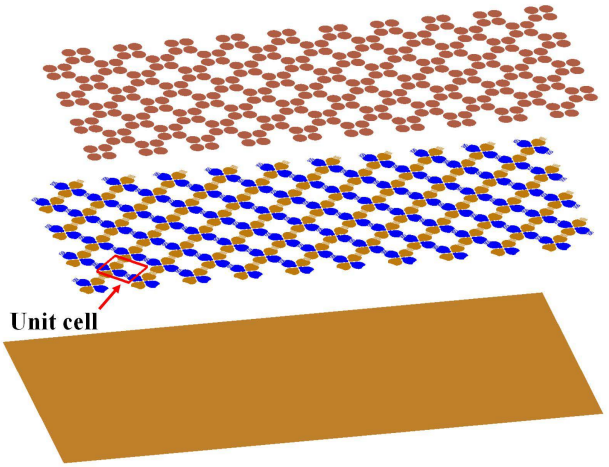

(a)

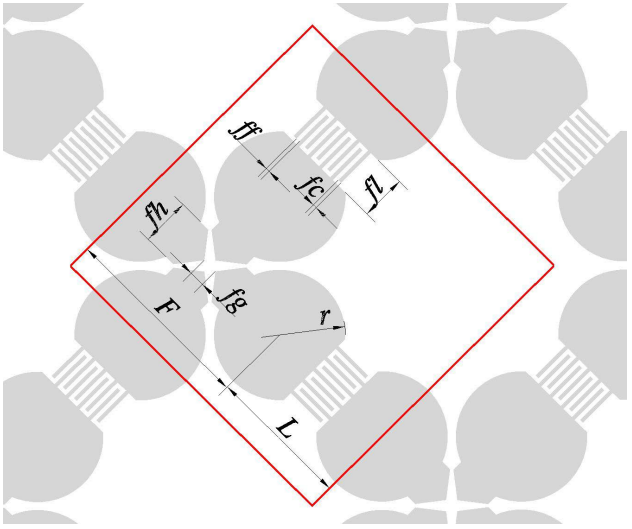

(b)

FIGURE 2. The planar array and its unit cell design before rolling up into a cylindrical array. The elements are dual polarized into ±45° orientation, (a) the exploded view of the finite array in planar form; (b) the unit cell for the finite array.

(or the ground plane) merely produces an inductance effect to the input terminals of the array. Bandwidth of the array can be expanded by introducing capacitors between the adjacent elements in the current sheet. This is due to the fact that the end tip capacitor can cancel out the short-circuit effect of the ground plane at the low frequency band. At the high frequency end, the dipole element in the array shows inductance characteristic, and the extra inductive effect introduced by the ground plane constrains the bandwidth of the array. Fig. 3 illustrates the input impedance of the four individual elements in the same array column, and other elements in the array exhibit similar input impedance characteristics as the elements in other columns are under similar boundary condition. The locations of elements "1," "2," "3" and "4" were shown in Fig. 1. The real part of the input impedance of element "1" is 28 Ω on average, which is smaller than the other three elements over the frequency range from 1.5 GHz to 6 GHz. However, the imaginary parts of the impedance for the four elements are closer to each other with a standard deviation of 5.6 Ω for the elements "2," "3," and "4." The reactance values are negative below 4.5 GHz, which demonstrates the capacitive nature of dipole elements at lower frequencies. In order to yield broader frequency bandwidth, mutual coupling between elements in the array is crucial.

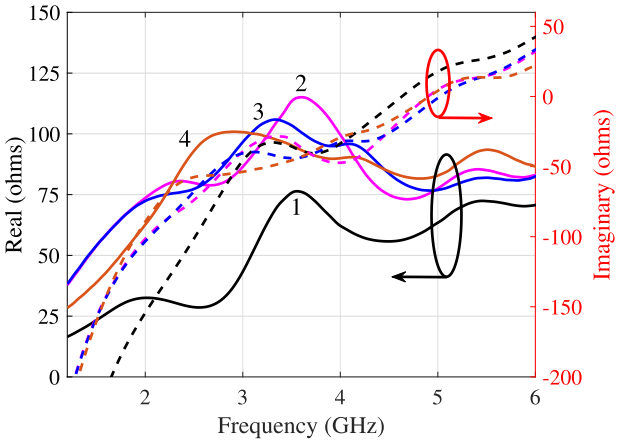

FIGURE 3. The input impedance of the elements in the cylindrical array as shown in Fig. 1, where the element "1" is at the bottom of the cylinder, the elements "2" and "3" are in the middle, and the element "4" is at the top of the cylinder near the edge. The real part of the impedance is associated with the *y*-axis on the left, the imaginary part the *y*-axis on the right.

In a tightly coupled array, mutual coupling can be constructively utilized to achieve a stable active impedance over a broad frequency bandwidth, and a sinusoidal current distribution has to be maintained at each frequency. Since the size of each element is approximately half-wavelength ($\lambda/2$) of the highest frequency of the band, its size is too small to radiate at the low frequency end. Therefore, in order to operate at lower frequencies, mutual coupling is the key to achieve the desired current distribution. However, mutual coupling between the elements in a cylindrical array is different compared to a planar array as a result of bending on the elements. The mutual coupling between the center element "3" and its surrounding elements in both the cylindrical array configuration and the corresponding planar array is shown in Fig. 4. It shows that the effect of mutual coupling in the cylindrical array is less distributive than the one in the planar array configuration. The average mutual coupling between the center element and the surrounding elements was −12 dB in the cylindrical array whereas −8 dB mutual coupling at 3 GHz between adjacent elements was observed in the planar array.

Furthermore, this distinction can be reflected by studying the active input impedance characteristics. A 3 × 3 subarray was investigated for the both array configu-

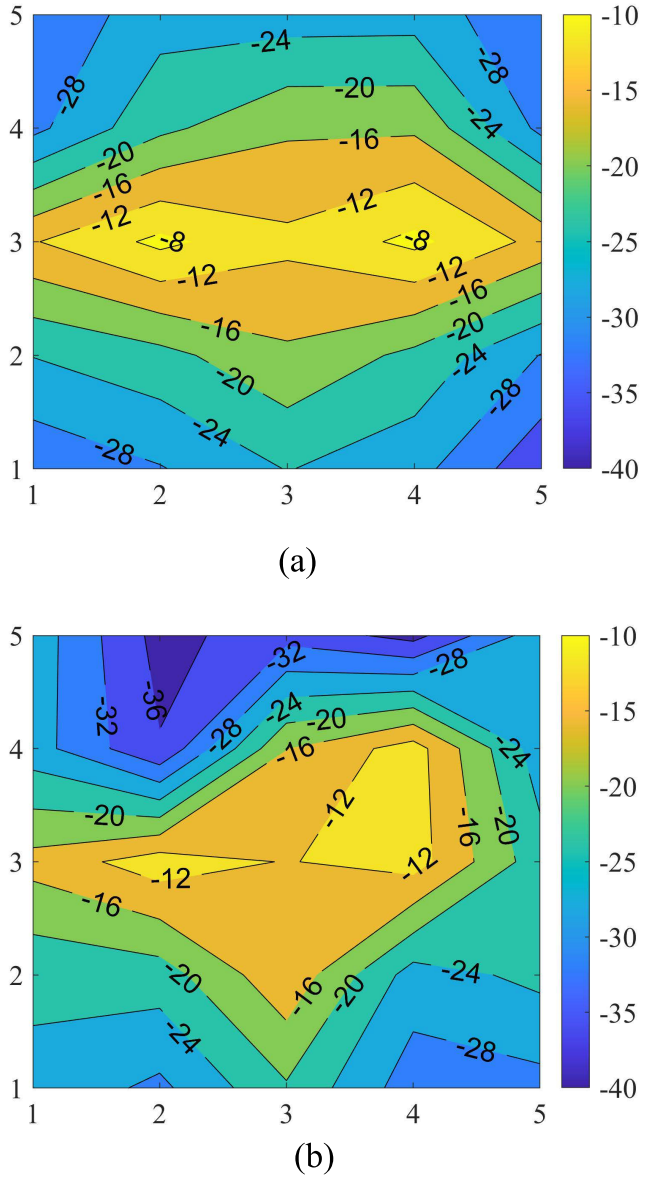

FIGURE 4. The mutual coupling at 3 GHz between the elements in two sub-arrays, labeled numbers in $x-$ and $y-$ axis represent the element number in a 5 × 5 subarray, (a) the mutual coupling for the elements in the cylindrical sub-array; (b) the mutual coupling for the elements in the corresponding planar sub-array. The element number "3" is at the center of a column in the cylindrical array, and at the center of the corresponding finite planar array.

rations, and the centre element in the 3 × 3 subarray was considered as the reference element. First, the active reflection coefficient was obtained based on scattering parameters [7],

$$\Gamma_{act}^{n} = \sum_{m=1}^{N} S_{nm}^{ant} \tag{2}$$

where n denotes the middle element of 3 × 3 subarray, N is equal to 9 representing the total number of the elements in the subarray. Then, the active input impedance of the central

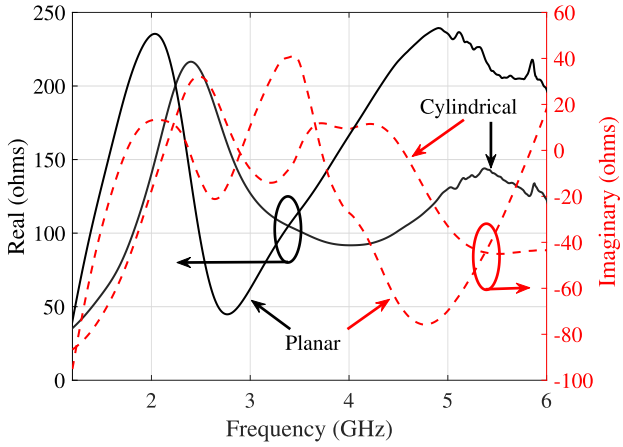

FIGURE 5. The active input impedance of the element "3" when the 8 adjacent elements become active with it together. The real and imaginary part of active input impedance for the element "3" are calculated considering all the mutual coupling with other 8 elements around it in both planar and cylindrical arrays.

TABLE 1. Geometric parameters for the unit cell design.

Parameter	Value (mm)	Description
L	11	Separation between discs in one element
F	15	Disc separation of neighboring elements
r	5	radius of the circular disc
fg	1.2	Gap for feed
fh	3.75	Feed strip width
fc	0.3	Finger width
ff	0.3	Finger gap
fl	3.5	Length of the finger

element of the subarray can be calculated by

$$Z_{act}^{n} = Z_0 \frac{1 + \Gamma_{act}^{n}}{1 - \Gamma_{act}^{n}}, \tag{3}$$

where Z_0 is the characteristic input impedance of the array element, which is 120 Ω for the crossed disc dipole design in this study. The active input impedance of the element of interest in the subarray within the cylindrical array and planar array is given in Fig. 5. The active reactance part of the impedance for the element in the cylindrical array were closer to zero at the low frequency than the element in the planar array, which further enhances the bandwidth towards the low frequency end. More specifically, the reflection coefficient is less than −15 dB for the center element in the cylindrical array at 1.7 GHz and above, it is less than −15 dB from 2.5 GHz and above in the case of planar array. In addition to the constructive mutual coupling effect in the tightly coupled array, the metasurface placed above the array was another important factor contributing to increasing the bandwidth. This is investigated in the following section.

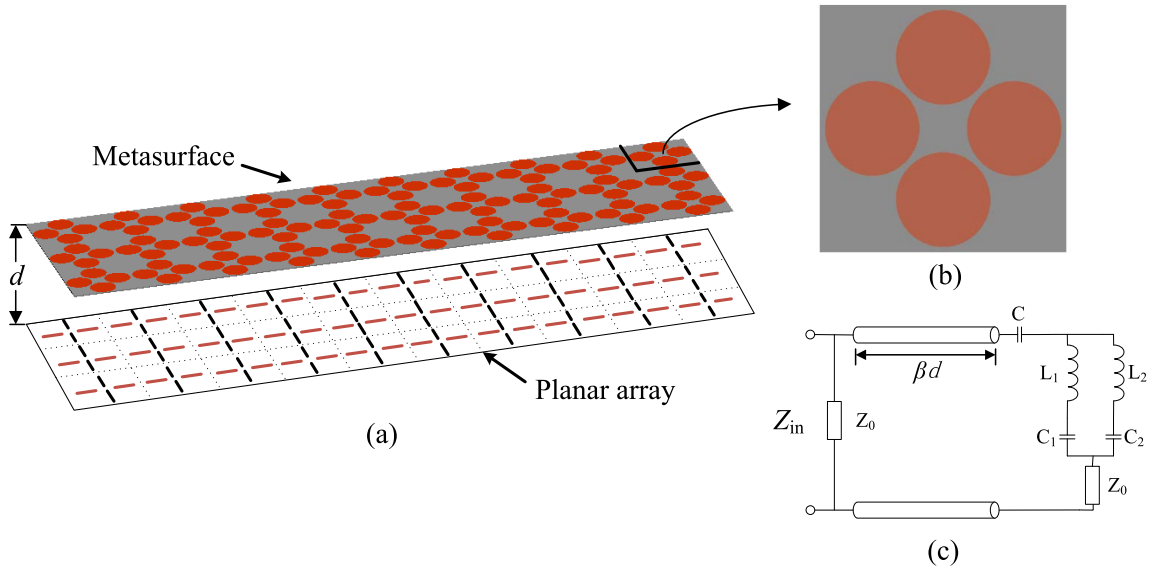

FIGURE 6. The equivalent circuit model for the metasurface, (a) metasurface and its relative position to the array; (b) the unit cell for the metasurface; (c) the equivalent circuit of the metasurface, Z_0 is the wave impedance of free space, d is the separation between array plane and metasurface.

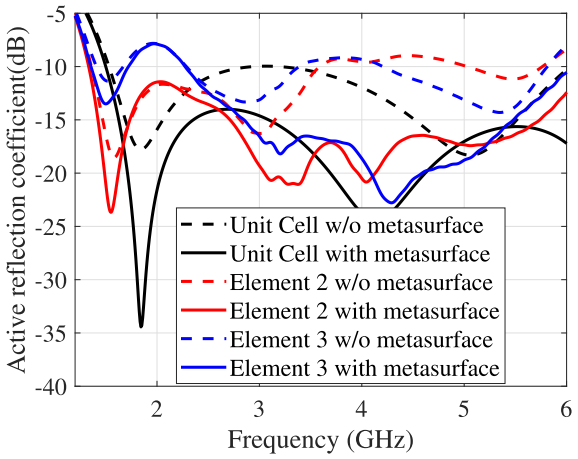

FIGURE 7. The active reflection coefficients of the elements in the arrays are compared, including an unit cell in the infinite planar array, and the embedded element "2" and "3" in the cylindrical array, under two configurations of with and without metasurface over the antenna arrays.

TABLE 2. Parameters for the cylindrical array design.

Parameter	Value (mm)	Description
$D1$	75	Diameter of ground plane cylinder
$D2$	117	Diameter of the active layer cylinder
$D3$	131	Diameter of the metamaterial layer cylinder
H	116	Height of the cylindrical array

B. METAMATERIAL WAIM

The use of innovative metamaterial and metasurface as coatings in antenna arrays can increase the bandwidth, enhance wide-scan capability or manipulate polarization status. For the tightly coupled dipole array configuration, the designed metasurface is based on conductive disks that are laid out on a thin sheet to achieve a wider bandwidth covering the entire sub-6GHz band, and it is placed above the planar array. The metasurface, the unit cell, and its equivalent circuit model are shown in Fig. 6. The disks were scattered following the same pattern as the array elements and finally form a metasurface. It is working as an impedance transformer between freespace and the feeding terminals of the antenna elements. Consequently, a broader frequency bandwidth is achieved. The effectiveness of the metasurface is clearly shown by observing the improvement on the reflection coefficient of the array element as shown in Fig. 7. Both the elements in the infinite planar array and the elements in the cylindrical array demonstrated a significant improvement (reflection coefficient changed from −10 dB to −15 dB on average) on impedance matching with the added metasurface. Fig. 6 (c) gives the Equivalent Circuit Model (ECM) for the metasurface, where βd denotes the distance from the metasurface to the plane of the array. When the radius of disk is 7 mm, the separation between the disks for one polarization is 20 mm, and the size of unit cell is 40 mm, the values of components for the ECM of the metasurface layer are summarized in Table 3.

C. RADIATION PATTERN CHARACTERISTICS

The co-polar radiation patterns of the cylindrical array are given in Fig. 8. The gain stability of the cylindrical array in the horizontal plane is high, and the variance of the gains over horizontal angles for the frequencies of 1.7 GHz, 2.5 GHz, 3.4 GHz, 4 GHz and 5.9 GHz are within 2 dB range, as expected. There are more fluctuations at the high frequency

TABLE 3. Values of ECM components for the metasurface.

Parameter	Value	Description
C	0.5 pF	capacitance
L_1	6 nH	inductance 1
C_1	0.05 pF	capacitance 1
L_2	10 nH	inductance 2
C_2	0.005 pF	capacitance 2
d	7 mm	separation from metasurface to the array
Z_0	377 Ω	wave impedance of free space

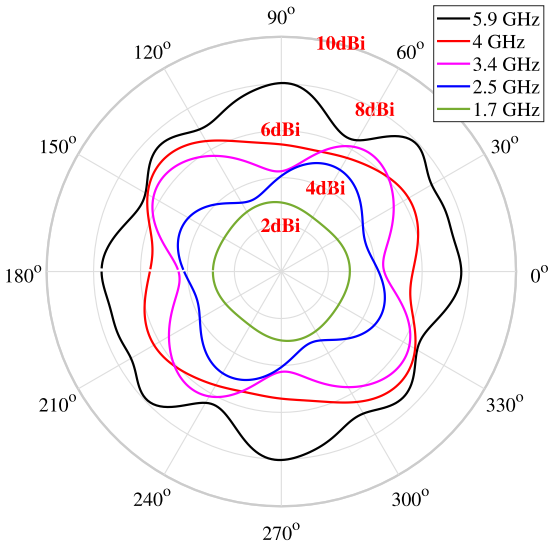

FIGURE 8. The co-polar directivity pattern of the cylindrical array in the horizontal plane, the radiation directivity is calculated when all of its 80 elements for one polarization, the +45°, are excited simultaneously.

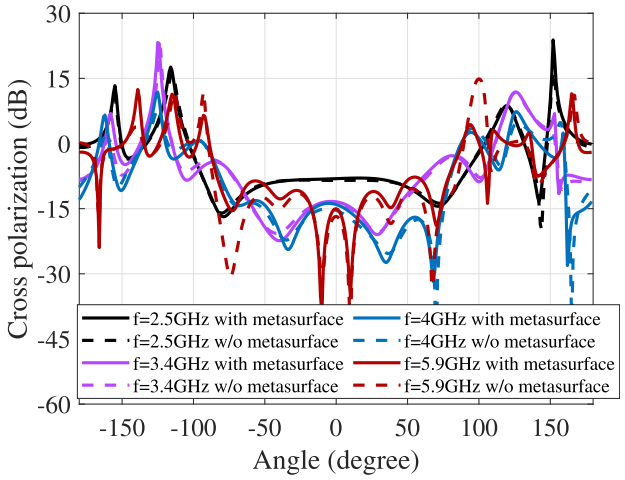

FIGURE 9. The cross polarization of the centre element in the cylindrical array, the ratio between the cross-polar and co-polar components of the far-field radiation for the element "3," under the configurations of with and without the metamaterial layer in the cylindrical array. All the other elements were terminated with matched loads apart from the element "3."

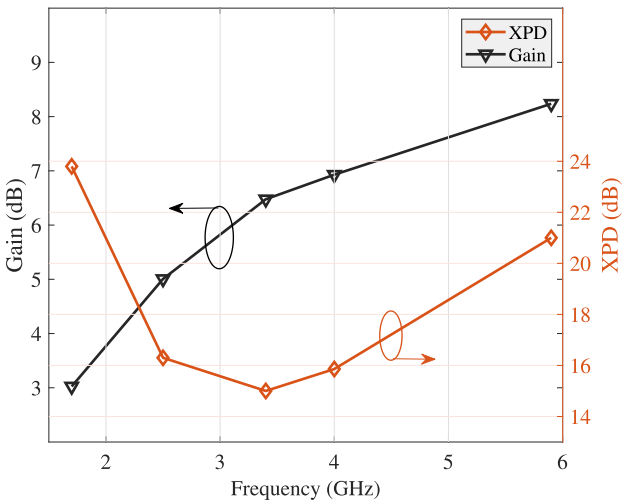

FIGURE 10. The realized gain and XPD of the cylindrical array in azimuth plane when all 80 elements of +45° polarization were simultaneously excited.

end, nevertheless they are still well within 2 dB. The XPD is greater than 15 dB for the cylindrical array radiation in the azimuth. It is worth mentioning that the cross polarization performance of the array is somewhat different from that for a single element excitation. The XPD performance of an element (element 3) in the array is shown in Fig. 9. The XPD is the lowest at 2.5 GHz in the frequency band of interest, where it is slightly less than 10 dB. It is noted that the metasurface has a minor effect on the polarization status, especially in the main direction, where $\theta = 0°$. However, in the case of array, all elements become active, therefore XPD is greater than 15 dB for each frequency monitored over the entire Sub-6 GHz band. Fig. 10 shows the gain and XPD of the entire cylindrical array when all elements for one polarization were excited. The gain varies between 3 and 8 dB, and the XPD is in the range of 15 dB to 24 dB through the sub-6 GHz band.

D. THE FEED NETWORK FOR ARRAY ELEMENTS

This study focuses on characterizing the slant polarized cylindrical array. Therefore, flexible coplanar waveguide (CPW) feed network was designed to access the elements externally for measurements. The fundamental structure to form the tightly coupled dipole array is balanced, and the elements are spreading over the ground plane with the distance of a quarter of wavelength at the highest frequency of the operational band. In this study, for the planar array, the optimal distance between the antenna elements and the ground plane is 16 mm, and it is 21 mm for the cylindrical array. The feed lines to extend the feed points from the surface of the tightly coupled dipoles to the points at the ground plane can introduce common mode resonance in the structure. To reduce this common mode resonance, flexible coplanar waveguides (CPW) were designed to feed the broadband dipole elements. The illustration of the design and the prototype for measurements are shown in Fig. 11 and Fig. 12,

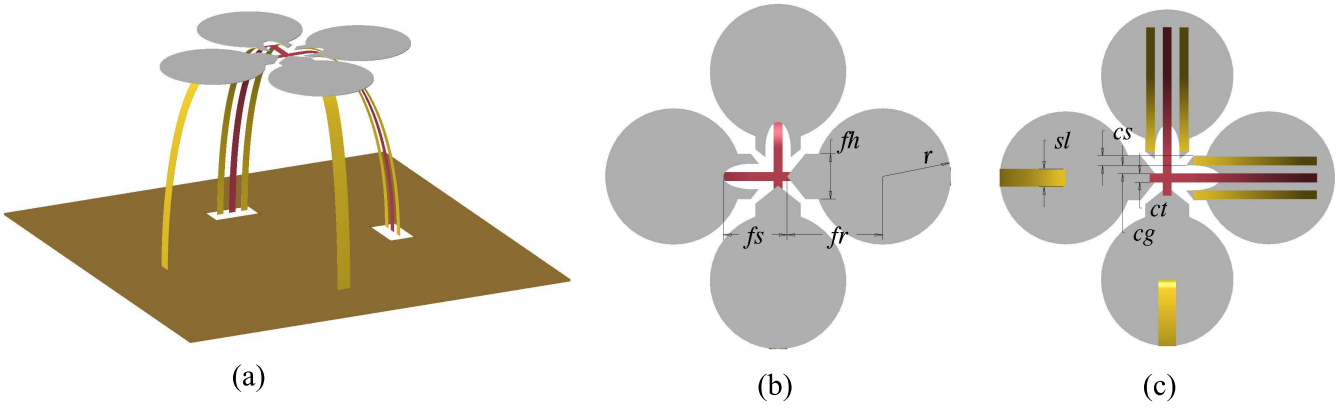

FIGURE 11. The illustration of the CPW feed design based on flexible material for the dual polarized crossed disk dipole antenna.

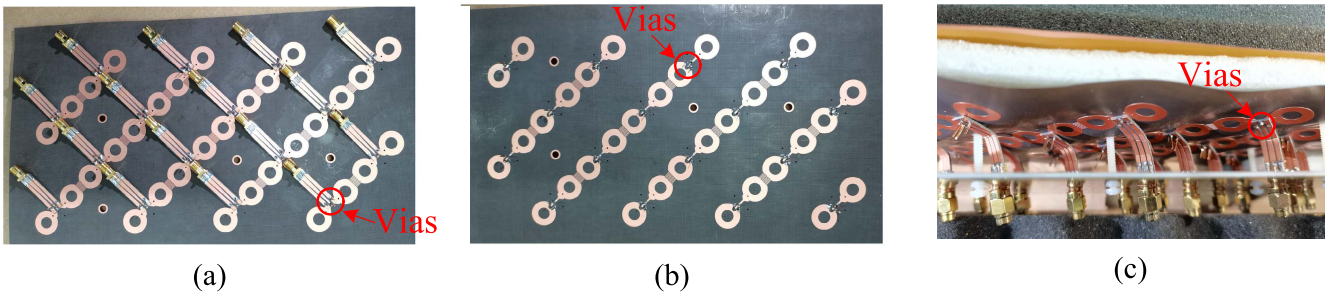

FIGURE 12. The CPWs to feed the crossed ring antenna, (a) the view from the bottom of planar array; (b) the view from the top of the planar array; (c) the CPWs were connected to the crossed disk dipole elements on the other side of board.

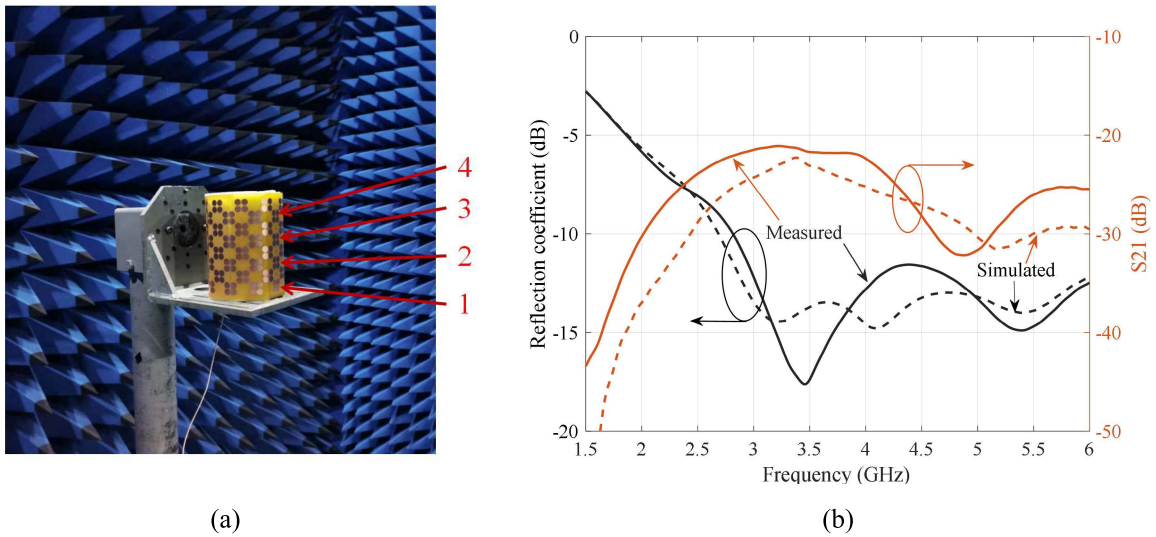

FIGURE 13. The cylindrical array prototype for characterization, the reflection coefficient and port isolation for dual polarization. (a) The cylindrical array in the anechoic chamber. (b) The reflection coefficient for the element "3" in the array, and isolation between the two dual polarized ports for the element "3."

where it can be seen that each element is fed through a CPW line terminated with an SMA connector. A parity strip is needed to eliminate the common mode propagation in the feeding structure, and this was investigated in greater details in [32]. If the parity strip is absent, and when the total length of the CPW is approximately half the wavelength, a resonance will occur at the corresponding frequency that is within the operational frequency band. The total length of the arch formed by the CPW and the parity strip is expected to be less than a wavelength of the highest frequency. It has

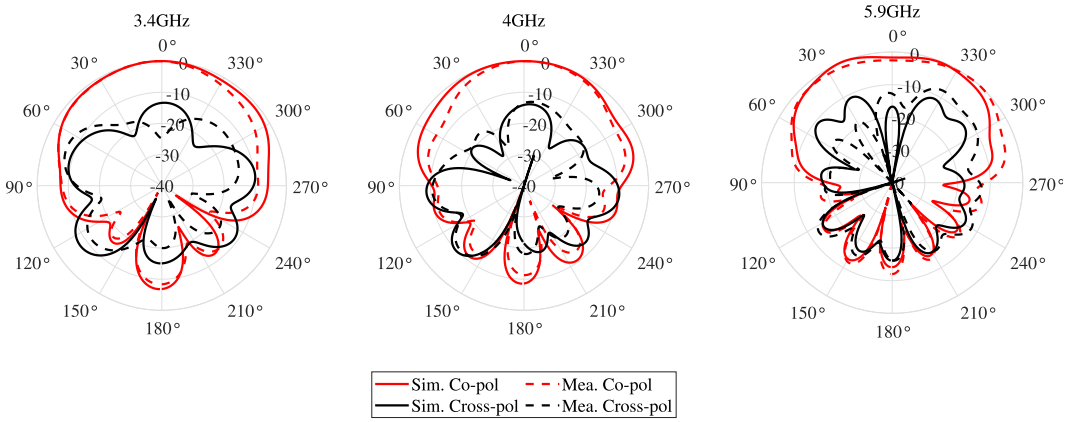

FIGURE 14. The radiation pattern of the element "3" in the cylindrical array shown in Fig. 13 when the rest elements of the cylindrical array are terminated in matched loads, three frequencies are shown, 3.4 GHz, 4 GHz and 5.9 GHz.

been verified in [32] that the effect from the bending of the CPW board on the wave propagation through the CPW was negligible. The CPW lines made from flexible materials offers a simple feeding approach, potentially leading to the realization of a fully printed phased array, where planar array and feed are fully printed and connected through vias.

III. MEASUREMENT AND VERIFICATION

The cylindrical array of ±45° slant polarization was fabricated and measured. The fabricated prototype model is shown in Fig. 13(a). The active layer and the metasurface are made from two types of substrates. The substrate for the active layer is 0.254 mm in thickness and the relative permittivity is 2.55 (Rogers AD255C, $\tan\delta = 0.0014$). The dual-polarized elements of the array are chemically etched on the opposite sides of the same board. The thickness of the substrate for the metasurface is PI (Polyimide) of 25 μm in thickness and the relative permittivity is 4.1 (PMTK182518JBB). The disks for the metasurface are chemically etched on one side of the thin PI sheet. The CPWs were manufactured by using PTFE based F_4BM-2-A255 ($\varepsilon_r = 2.55$, $\tan\delta = 0.0015$) with the thickness of 0.3 mm. The separation between the metasurface and the active layer is 7 mm, which is the same for both the planar array and the cylindrical array. The optimal spacing between the active layer and the ground plane is 16 mm for the planar array and 21 mm for the cylindrical array, which is corresponding to a quarter wavelength at 4.7 GHz and 3.6 GHz, respectively. For the planar array before wrapping up into a cylindrical array, the element spacing is 26 mm, which is half a wavelength at 5.8 GHz. Considering the desired highest operational frequency of 5.9 GHz for the proposed array, 26 mm is 0.51 times of the wavelength, which is slightly more than a half wavelength. The cylindrical array can be extended vertically for higher gains, the current form of 116 mm in height, that is approximately one wavelength at the highest frequency. This height is chosen to accommodate the minimum number of elements so that the input impedance of the centre element in the cylindrical array becomes stable (i.e., the active reflection coefficient was less than −10 dB over the entire frequency band). With this size, there are four rows of elements in each column, and 20 columns together in the array. This array configuration was adopted for several factors and will be discussed in more details in the next section.

The reflection coefficient for the element 3 is shown in Fig. 13(b) where the results from measurement and simulation were compared when all the other elements in the cylindrical array were terminated with matched loads. It indicates that the embedded element in the cylindrical array can operate effectively from 2.75 GHz and above without exciting the neighboring elements. The isolation between ports of dual polarization is more than 20 dB. Moreover, the radiation patterns for the center element have been measured. Radiation pattern was measured for element "3" as shown in Fig. 1, Fig. 14 compares the measured and calculated co-polar and cross-polar patterns in the horizontal plane for element "3." Simulation results were compared with measured results at the higher frequencies 3.4 GHz, 4 GHz, and 5.9 GHz where the reflection coefficient for the observed element was less than −10 dB without requiring excitation on neighboring elements. The XPD is over 15 dB in the horizontal plane for all three frequencies observed at boresight direction. At the high end of the frequency, i.e., 5.9 GHz, the cross polarization rises at wide angles. Nevertheless, it is approximately 10 dB lower than the copolar component within 60° off the boresight direction.

IV. DISCUSSION

The tightly coupled wideband circular dipole array with ±45° polarization was successfully realized on a cylindrical surface. The array produces omnidirectional radiation pattern in azimuth plane with rotational symmetry characteristics. The proposed antenna array covers the sub-6 GHz (between 1.7 GHz and 5.9 GHz) frequency band for mobile communications. The cross polarization performance was

TABLE 4. Comparison of slant-polarized antenna and arrays for communication.

Design	Shape	Bandwidth	Coverage	Gain	XPD	Isolation	Ports
[19]	Planar	45% (1.71-2.69 GHz)	Directional (3 dB beamwidth 65°)	8.5 dB	20 dB	25 dB	2 ports with dual polarization
[20]	Cylindrical	22% (1.75-2.18 GHz)	Omnidirectional	0dB (Variation 1 dB)	15dB	NA	4 dual-polarized elements
[33]	Cylindrical	37% (1.85-2.69 GHz)	Omnidirectional	2 dBi (Variation 2 dB)	10 dB	NA	4 single polarized elements
[34]	Planar	47% (1.7-2.75 GHz)	Directional (3 dB beamwidth 65°)	9 dBi	25 dB	45 dB	2 ports with dual polarization
[35]	Sectoral	4% (5.15-5.35 GHz)	Directional (3 dB beamwidth 60°)	15 dBi	NA	NA	2 ports with 36 elements
[36]	Planar	45% (1.7-2.7 GHz)	Directional (3 dB beamwidth 37°)	2.4-6 dBi	35 dB	40 dB	2 ports for 4 elements
This Work	Cylindrical	110% (1.7-5.9 GHz)	Omnidirectional	8dB (Variation 2 dB)	15 dB	20 dB	80 dual-polarized elements (160)

satisfactory with XPD lower than −15 dB at boresight over the entire frequency range. In addition to these features, it was demonstrated that the mutual coupling among elements in the cylindrical array was more concentrated than in the case of planar array. Hence elements in a small subarray of 3×3 can achieve a reasonable impedance matching and a combination of many subarrays can then be established from the cylindrical array to steer multiple independent beams. This is one of the reasons to have 80 ports per polarization in the design to study the properties of the cylindrical array. There are several factors that have been considered to determine the size of the array: (1) solid impedance matching for elements in the array requires at least 3 elements in one column; (2) to achieve a reasonable gain in the elevation plane: 4 elements in one column was a good compromise to have the right value with a minimum number of elements; (3) space is needed at the axis region of the cylinder for element accessing. Hence, the diameter for the ground plane cylinder was an important factor to consider the number of columns. Having many ports, i.e., two ports for each dual polarized element, enables the proposed cylindrical array to be implemented in massive MIMO communications or radar imaging applications, where each antenna must be connected to a separate RF chain for maximum performance. Finally, the CPW feed lines made from thin material for feeding elements on curved surface can be further explored to realize entirely printed low cost phased arrays. The proposed cylindrical array design was compared with other reported antenna and array designs of linear slant-polarization in Table 4. The ultra-wide frequency bandwidth of the new design is distinct to other existing designs. Another important feature is that many ports offered by the proposed cylindrical array design can be employed to form multiple beams simultaneously to perform precise beamforming. This shall be attractive to certain applications where flexibility is needed in the front-end subsystem, e.g., massive MIMO and phased array radar applications. It is worth mentioning that the previous studies on slant-polarized arrays have focused on applications for the past wireless communication systems where directional radiation was dominating and multi-beam capability was yet to be implemented. The large number of ports with ultra-wideband capability offered by the proposed design will potentially meet the requirement of the next generation wireless networks, where sensing and communication are expected to be integrated within the same system.

V. CONCLUSION

A slant-polarized omnidirectional cylindrical array antenna has been designed and developed by utilizing tightly coupled dipole antenna elements of ±45° polarization. 80 dual-polarized elements were arranged in a cylindrical form consisting of 4 circular rows and 20 vertical columns. The main characteristics of the cylindrical array were investigated and compared to the corresponding planar array. A bandwidth of 110% (1.7-5.9 GHz) was obtained with the criteria of 10 dB return loss. It produces an omnidirectional radiation pattern in the azimuth plane with a gain variation of 2 dB at any frequency over its entire bandwidth. The cross-polarization at boresight was below −15 dB over the entire sub-6 GHz frequency band. The rotational symmetry of the radiation patterns in the azimuth plane was achieved due to geometrical symmetry between the ±45° polarized elements with respect to the horizontal plane. The proposed ultra-wideband array antenna design and the demonstrated performance offer a great flexibility to be used for a wide range of applications. It can be excited simultaneously for omnidirectional coverage or grouped into sub-arrays for multi-beam steering applications. In addition, size and number of elements can be easily adjusted to suite specific applications. Furthermore, the low profile and ease of manufacturing offer an additional advantage. Therefore, the proposed design is a promising solution for future wireless, radar and communication systems.

ACKNOWLEDGMENT

The authors would like to express their gratitude to Prof. Jianxin Chen and Prof. Wenwen Yang for their help on the measurements.

REFERENCES

[1] H. Wu, M. Ravan, and R. K. Amineh, "Holographic near-field microwave imaging with antenna arrays in a cylindrical setup," *IEEE Trans. Microw. Theory Techn.*, vol. 69, no. 1, pp. 418–430, Jan. 2021.

[2] Y. Liu, H. Yang, Z. Jin, F. Zhao, and J. Zhu, "A multibeam cylindrically conformal slot array antenna based on a modified Rotman lens," *IEEE Trans. Antennas Propag.*, vol. 66, no. 7, pp. 3441–3452, Jul. 2018.

[3] W. Hong, Z. H. Jiang, C. Yu, J. Zhou, P. Chen, Z. Yu, H. Zhang, B. Yang, X. Pang, M. Jiang, Y. Cheng, M. K. T. Al-Nuaimi, Y. Zhang, J. Chen, and S. He, "Multibeam antenna technologies for 5G wireless communications," *IEEE Trans. Antennas Propag.*, vol. 65, no. 12, pp. 6231–6249, Dec. 2017.

[4] Y. Gao, R. Ma, Y. Wang, Q. Zhang, and C. Parini, "Stacked patch antenna with dual-polarization and low mutual coupling for massive MIMO," *IEEE Trans. Antennas Propag.*, vol. 64, no. 10, pp. 4544–4549, Oct. 2016.

[5] B. Mohamadzade, R. B. V. B. Simorangkir, R. M. Hashmi, R. Gharaei, A. Lalbakhsh, S. Shrestha, M. Zhadobov, and R. Sauleau, "A conformal, dynamic pattern-reconfigurable antenna using conductive textile-polymer composite," *IEEE Trans. Antennas Propag.*, vol. 69, no. 10, pp. 6175–6184, Oct. 2021.

[6] E. Crespo-Bardera, A. G. Martin, A. Fernandez-Duran, and M. Sanchez-Fernandez, "Design and analysis of conformal antenna for future public safety communications: Enabling future public safety communication infrastructure," *IEEE Antennas Propag. Mag.*, vol. 62, no. 4, pp. 94–102, Aug. 2020.

[7] S. Xiao, S. Yang, H. Zhang, Q. Xiao, Y. Chen, and S.-W. Qu, "Practical implementation of wideband and wide-scanning cylindrically conformal phased array," *IEEE Trans. Antennas Propag.*, vol. 67, no. 8, pp. 5729–5733, Aug. 2019.

[8] M. Golmohamadi, A. Narbudowicz, and J. Frolik, "Mitigating indoor channels with quad-polarization diversity," *IEEE Antennas Wireless Propag. Lett.*, vol. 18, no. 6, pp. 1199–1202, Jun. 2019.

[9] B. Lindmark and M. Nilsson, "On the available diversity gain from different dual-polarized antennas," *IEEE J. Sel. Areas Commun.*, vol. 19, no. 2, pp. 287–294, Feb. 2001.

[10] H. A. Wheeler, "Simple relations derived from a phased-array antenna made of an infinite current sheet," *IEEE Trans. Antenna Propag.*, vol. AP-13, no. 4, pp. 506–514, Jul. 1965.

[11] B. Munk, R. Taylor, T. Durharn, W. Croswell, B. Pigon, R. Boozer, S. Brown, M. Jones, J. Pryor, S. Ortiz, J. Rawnick, K. Krebs, M. Vanstrum, G. Gothard, and D. Wiebelt, "A low-profile broadband phased array antenna," in *Proc. IEEE Antennas Propag. Soc. Int. Symp.*, Columbus, OH, USA, vol. 2, Jun. 2003, pp. 448–451.

[12] Y. Zhang and A. K. Brown, "Octagonal ring antenna for a compact dual-polarized aperture array," *IEEE Trans. Antennas Propag.*, vol. 59, no. 10, pp. 3927–3932, Oct. 2011.

[13] A. B. Munk, "Broadband wire arrays," in *Finite Antenna Arrays and FSS*. New York, NY, USA: Wiley, 2003, ch. 4, pp. 181–214.

[14] Y. Zhang and A. K. Brown, "A wideband planar aperture array using interconnected crossed rings," *IEEE Trans. Antennas Propag.*, vol. 67, no. 2, pp. 945–950, Feb. 2019.

[15] H. Zhang, S. Yang, S. Xiao, Y. Chen, and S. Qu, "Low-profile, lightweight, ultra-wideband tightly coupled dipole arrays loaded with split rings," *IEEE Trans. Antennas Propag.*, vol. 67, no. 6, pp. 4257–4262, Jun. 2019.

[16] G. Oliveri, A. Polo, M. Salucci, G. Gottardi, and A. Massa, "SbD-based synthesis of low-profile WAIM superstrates for printed patch arrays," *IEEE Trans. Antennas Propag.*, vol. 69, no. 7, pp. 3849–3862, Jul. 2021.

[17] S. Sajuyigbe, M. Ross, P. Geren, S. A. Cummer, M. H. Tanielian, and D. R. Smith, "Wide angle impedance matching metamaterials for waveguide-fed phased-array antennas," *IET Microw., Antennas Propag.*, vol. 4, no. 8, pp. 1063–1072, 2010.

[18] J. J. A. Lempiainen and J. K. Laiho-Steffens, "The performance of polarization diversity schemes at a base station in small/micro cells at 1800 MHz," *IEEE Trans. Veh. Technol.*, vol. 47, no. 3, pp. 1087–1092, Aug. 1998.

[19] Y. Luo, Q.-X. Chu, and D.-L. Wen, "A plus/minus 45 degree dual-polarized base-station antenna with enhanced cross-polarization discrimination via addition of four parasitic elements placed in a square contour," *IEEE Trans. Antennas Propag.*, vol. 64, no. 4, pp. 1514–1519, Apr. 2016.

[20] X. Quan, R. Li, Y. Fan, and D. E. Anagnostou, "Analysis and design of a 45° slant-polarized omnidirectional antenna," *IEEE Trans. Antennas Propag.*, vol. 62, no. 1, pp. 86–93, Jan. 2014.

[21] J.-K. Che, C.-C. Chen, and J. F. Locke, "A compact four-channel MIMO 5G sub-6 GHz/LTE/WLAN/V2X antenna design for modern vehicles," *IEEE Trans. Antennas Propag.*, vol. 69, no. 11, pp. 7290–7297, Nov. 2021.

[22] M. A. Jensen and J. W. Wallace, "A review of antennas and propagation for MIMO wireless communications," *IEEE Trans. Antennas Propag.*, vol. 52, no. 11, pp. 2810–2824, Nov. 2004.

[23] M. Temiz, E. Alsusa, L. Danoon, and Y. Zhang, "On the impact of antenna array geometry on indoor wideband massive MIMO networks," *IEEE Trans. Antennas Propag.*, vol. 69, no. 1, pp. 406–416, Jan. 2021.

[24] X. Gao, O. Edfors, F. Rusek, and F. Tufvesson, "Massive MIMO performance evaluation based on measured propagation data," *IEEE Trans. Wireless Commun.*, vol. 14, no. 7, pp. 3899–3911, Jul. 2015.

[25] J. Gilmore and D. B. Davidson, "Suppressing undesired common-mode resonances in connected antenna arrays," *IEEE Trans. Antennas Propag.*, vol. 63, no. 11, pp. 5245–5250, Nov. 2015.

[26] Y. Li, S. Xiao, C.-H. Hu, and Z. Yao, "A low-profile light-weight wideband connected parallel slot array for wide-angle scanning," *IEEE Trans. Antennas Propag.*, vol. 68, no. 2, pp. 813–823, Feb. 2020.

[27] Z. Tang, J. Liu, R. Lian, Y. Li, and Y. Yin, "Wideband differentially fed dual-polarized planar antenna and its array with high common-mode suppression," *IEEE Trans. Antennas Propag.*, vol. 67, no. 1, pp. 131–139, Jan. 2019.

[28] D. Cavallo, A. Neto, G. Gerini, A. Micco, and V. Galdi, "A 3-to 5-GHz wideband array of connected dipoles with low cross polarization and wide-scan capability," *IEEE Trans. Antennas Propag.*, vol. 61, no. 3, pp. 1148–1154, Mar. 2013.

[29] J. Zhong, A. Johnson, E. A. Alwan, and J. L. Volakis, "Dual-linear polarized phased array with 9:1 bandwidth and 60° scanning off broadside," *IEEE Trans. Antennas Propag.*, vol. 67, no. 3, pp. 1996–2001, Mar. 2019.

[30] W. Zhou, Y. Chen, and S. Yang, "Dual-polarized tightly coupled dipole array for UHF-X-band satellite applications," *IEEE Antennas Wireless Propag. Lett.*, vol. 18, no. 3, pp. 467–471, Mar. 2019.

[31] A. O. Boryssenko, "Polarization constraints in dual-polarized phased arrays derived from an infinite current sheet model," *IEEE Antennas Wireless Propag. Lett.*, vol. 8, pp. 955–958, 2009.

[32] X. Lv, Y. Zhang, Q. Shi, Y. Fu, H. Xing, H. Peng, and M. Temiz, "Dual function flexible coplanar waveguide for feeding antenna of balanced structure," in *Proc. Int. Symp. Antennas, Propag. EM Theory (ISAPE)*, Zhuhai, China, Dec. 2021, pp. 1–3.

[33] H. Arai, B. Rohani, and R. Kaneda, "Slant 45° polarized multi-frequency cylindrical slot-dipole antenna," in *Proc. 6th Asia–Pacific Conf. Antennas Propag. (APCAP)*, Oct. 2017, pp. 1–3.

[34] Y. Cui, X. Gao, and R. Li, "A broadband differentially fed dual-polarized planar antenna," *IEEE Trans. Antennas Propag.*, vol. 65, no. 6, pp. 3231–3234, Jun. 2017.

[35] M. Hajj, R. Chantalat, T. Monédière, and B. Jecko, "A 45° linearly polarized sectoral antenna with M-EBG structure for WiMAX base stations," *IEEE Antennas Wireless Propag. Lett.*, vol. 9, pp. 737–740, 2010.

[36] V. F. Fusco and P. H. Rao, "Wide-band dual slant linearly polarized antenna," *IEEE Trans. Antennas Propag.*, vol. 51, no. 8, pp. 2014–2019, Aug. 2003.

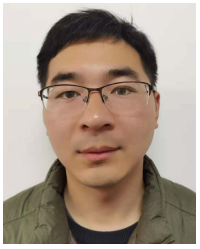

XIANYANG LV received the B.S. degree from the Nanjing Institute of Technology, Nanjing, China, in 2009, and the M.S. degree from Chongqing Jiaotong University, Chongqing, China, in 2012. He is currently pursuing the Ph.D. degree with the School of Information Science and Technology, Nantong University, Nantong, China. He is also working as a Lecturer with the School of Information Science and Technology, Nantong University, focusing on sensors for automatic transport vehicles. His current research interests include antenna array design using flexible material, multibeam scanning, and low-cost front-end techniques.

YONGWEI ZHANG (Member, IEEE) received the B.S. degree in communication engineering from Jilin University, in 1996, and the Ph.D. degree from the School of Electrical and Electronic Engineering, The University of Manchester, U.K., in 2007. In 1996, he joined Lucent Technologies (AT&T initially), China, where he was an Application Engineer on 5ESS® systems, and later a System Engineer and had been worked for Lucent, until 2003. While he was working for Lucent, in 1998, he was sent as a Visitor to the Bell Laboratories, Indian Hill, Naperville, IL, USA, trained in communication systems engineering tool development and later certified as an international instructor. In the years working for Lucent Technologies, from 1996 to 2003, he had been involved in 5ESS® switch application engineering and optimization for wireless communication systems. In 2003, he joined The University of Manchester first as a Ph.D. student and later a Research Fellow, then the Task Leader of the front-end design work package in Mid-Frequency Aperture Array Consortium for the Square Kilometre Array (SKA). His current research interests include antenna and array designs based on flexible material, electromagnetic theories, antenna array calibration techniques, and radio astronomy instrumentation.

QUAN SHI received the M.S. and Ph.D. degrees in management information systems from the University of Shanghai for Science and Technology, Shanghai, China, in 2005 and 2011, respectively. He is currently a Professor with the School of Transportation, Nantong University, China. His research interests include developments of signal and image processing and big data techniques.

MURAT TEMIZ (Member, IEEE) received the B.S. degree from Gazi University, Ankara, Turkey, in 2011, the M.S. degree from the TOBB University of Economics and Technology, Ankara, in 2013, and the Ph.D. degree from the Department of Electrical and Electronic Engineering, The University of Manchester, Manchester, U.K., in 2020. During his Ph.D. degree, he was also working as a Research Assistant focusing on massive multiple-input–multiple-output (MIMO) communication, MIMO orthogonal frequency-division multiplexing (OFDM) radars, and energy efficiency. His current research interests include massive MIMO systems, antenna array design, channel measurements, optimization, dual-functional MIMO OFDM radar communication systems, and machine learning applications.

AHMED EL-MAKADEMA received the B.S. degree in computing and communication systems engineering, the M.S. degree in communication engineering, and the Ph.D. degree in microwave and communication systems from The University of Manchester, in 2004, 2005, and 2011, respectively. He has been a member of the team working on the Square Kilometre Array (SKA) project since 2006. His primary research interests include wide band antenna, large antenna array design, beamforming, and electromagnetic computation and radars.